

# Evidence of Galaxy Expansion from Globular Clusters

Garen S. Karapetian<sup>1</sup>, Abraham P. Mahtessian<sup>1</sup>, Lev E. Byzalov<sup>2</sup>, Martik A. Hovhannisyan<sup>3</sup>, Lazar A. Mahtessian<sup>3</sup>

<sup>1</sup>Byurakan Astrophysical Observatory after V. Ambartsumian NAS of the Republic of Armenia, Byurakan, Republic of Armenia

<sup>2</sup>Faculty of Science, University of Waterloo, Ontario, Canada

<sup>3</sup>Institute of Applied Problems of Physics NAS of the Republic of Armenia 25 Hrachya Nersissian Str., Yerevan, Republic of Armenia

Email: amahtes@gmail.com

**How to cite this paper:** Karapetian, G.S., Mahtessian, A.P., Byzalov, L.E., Hovhannisyan, M.A. and Mahtessian, L.A. (2025) Evidence of Galaxy Expansion from Globular Clusters. *International Journal of Astronomy and Astrophysics*, 15, 121-138.  
<https://doi.org/10.4236/ijaa.2025.152009>

**Received:** April 4, 2025

**Accepted:** June 21, 2025

**Published:** June 24, 2025

Copyright © 2025 by author(s) and Scientific Research Publishing Inc.

This work is licensed under the Creative Commons Attribution International License (CC BY 4.0).

<http://creativecommons.org/licenses/by/4.0/>



Open Access

## Abstract

In modern astrophysics, it is believed that galaxies are not expanding. The authors of the article set out to investigate the motion of Globular Clusters (GC) of the Milky Way relative to the plane and center of the Galaxy. The study yielded the following results: 1. The average velocity of the GC relative to the Galactic plane for the northern region of the Galaxy has a positive value of approximately  $30.36 \pm 15.29$  km/s ( $N = 42$ ) for the range  $0^\circ < b < 13^\circ$ . 2. For the southern region, the following result was obtained: the average velocity of GC movement relative to the plane in the southern direction is  $-17.83 \pm 13.54$  km/s ( $N = 50$ ) for the range  $-13^\circ < b < 0^\circ$ . 3. The average velocity of the GC relative to the Galactic center for the range 0 to 12 kpc is  $31.70 \pm 14.74$  km/s ( $N = 119$ ). Thus, we can state that the Galaxy is possibly expanding, at least in its central part. This seems unlikely as it does not agree with the current theory, so it can be considered a preliminary result requiring further study. However, if we accept the idea of the expansion of the Galaxy, we can answer a number of questions. In particular, we can explain the existence of massive galaxies discovered by the James Webb Space Telescope (JWST), whose age is estimated to be less than 1 billion years.

## Keywords

Globular Clusters, Galactic Center, Galaxy Expansion

## 1. Introduction

As galaxies are not considered to be expanding, there are almost no papers devoted to this topic in the literature. A rare exception is the paper [1]. In this paper,

they explore the truncations in two nearby ( $D \sim 15$  Mpc) Milky Way-like galaxies: NGC 4565 and NGC 5907. The vertical extent of the truncation, as well as the colour properties in the mid-plane beyond the truncation, are consistent with an upper limit for the current growth speed for the discs of the galaxies of  $0.6 - 1$  kpc  $\text{Gyr}^{-1}$ , which corresponds to a speed of approximately  $500 - 1000$  m/s.

Our goal was to determine the expansion of the Galaxy by studying the motion of well-studied globular clusters.

The new Gaia Mission EDR3 and ED3 data represent improved parameters of the photometric and astrometric catalogs compared to previous versions. In particular, the inaccuracies in parallaxes  $\varpi$  and proper motions  $\mu$  were reduced on average by a factor of two, and systematic inaccuracies were reduced even more. Already DR2 has made it possible to calculate the average parallaxes ([2] [3]) and proper motions of almost all GC ([4]-[6]) of the Milky Way. Since GC stars have similar kinematic properties and parallaxes, [7] used these data sets (up to tens of thousands of stars in the richest clusters) to determine whether these stars belong to the GC and calculate their general parameters. Thus, a catalog of 164 GC with the necessary parameters was created, which we used to study the velocities of these GC relative to the plane  $V_{\uparrow}$  and  $V_{\downarrow}$  (north and south regions) and center ( $VR$ ) of the Milky Way Galaxy. First, we calculated the velocities of movement of all GC in the orthogonal direction relative to the plane for the northern and southern regions of the Galaxy. Further, in Section 2.1 we calculated the average GC movement velocities depending on the Galactic latitude  $b$ , and in Section 2.2, separately, on the distance of the GC to the Galactic plane. **Figure 1** and **Figure 2** show the dependence of GC velocities on galactic latitude for the northern and southern regions of the Galaxy. **Table 1** and **Table 2** summarize the main findings of the study.

## 2. Method

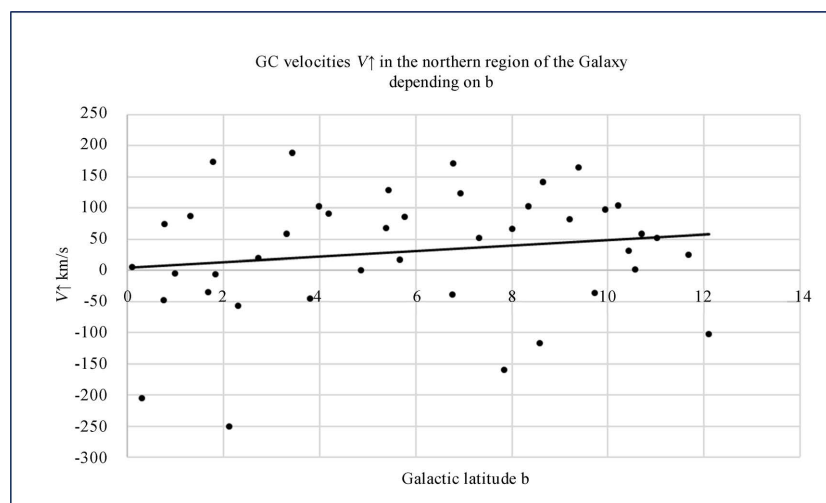


**Figure 1.** GC velocities  $V_{\uparrow}$  in the northern region of the Galaxy depending on coordinate  $b$ . As can be seen from the figure, most GCs have a positive velocity, *i.e.* moving away from the galactic plane.

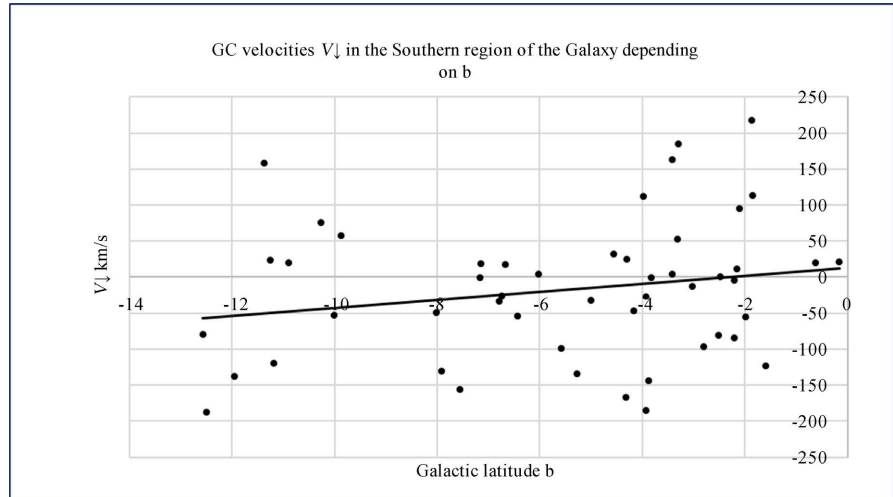


**Figure 2.** GC velocities  $V_{\downarrow}$  in the southern region of the Galaxy depending on coordinate  $b$ . Most GCs have a negative velocity, *i.e.* moving away from the galactic plane.

**Table 1.** The sample for  $-13^{\circ} < b < 13^{\circ}$  consists of 92 GCs.

| Name         | $RA$       | $DEC$      | $R_{sun}$ kpc | $b$ deg | $\mu l$ [mas yr $^{-1}$ ] | $\mu b$ [mas yr $^{-1}$ ] | $V_{\uparrow}, V_{\downarrow}$ km/s |
|--------------|------------|------------|---------------|---------|---------------------------|---------------------------|-------------------------------------|
| ESO_452-SC11 | 249.854167 | -28.399167 | 7.39          | 12.10   | -5.8677450                | -3.0835660                | -102.18                             |
| Rup_106      | 189.667500 | -51.150278 | 20.71         | 11.67   | -1.2716863                | 0.3370817                 | 24.67                               |
| NGC_6287     | 256.288904 | -22.708005 | 7.93          | 11.02   | -4.4497451                | 2.9439506                 | 52.34                               |
| NGC_6333     | 259.799086 | -18.516257 | 8.3           | 10.71   | -3.8819845                | 0.0400754                 | 59.27                               |
| NGC_5286     | 206.611710 | -51.374249 | 11.1          | 10.57   | 0.1481820                 | -0.1964969                | 1.27                                |
| NGC_6535     | 270.960449 | -0.297639  | 6.36          | 10.44   | -4.5564066                | 2.3670137                 | 31.31                               |
| NGC_6356     | 260.895804 | -17.813027 | 15.66         | 10.22   | -4.9125405                | 1.3039966                 | 103.88                              |
| NGC_6284     | 256.120114 | -24.764799 | 14.21         | 9.94    | -3.5101230                | 1.4025257                 | 98.06                               |
| NGC_6342     | 260.291573 | -19.587659 | 8.01          | 9.73    | -7.5343118                | -1.4921814                | -36.33                              |
| NGC_6273     | 255.657486 | -26.267971 | 8.34          | 9.38    | -0.6054084                | 3.6079414                 | 164.55                              |
| Ter_3        | 247.162483 | -35.339829 | 7.64          | 9.20    | -5.0790522                | 2.8935819                 | 81.81                               |
| NGC_3201     | 154.403427 | -46.412476 | 4.74          | 8.64    | 8.0250230                 | 3.0374465                 | 141.94                              |
| Gran_2       | 257.890000 | -24.849000 | 15.84         | 8.59    | -1.9641201                | -1.6698459                | -116.12                             |
| NGC_6779     | 289.148193 | 30.183472  | 10.43         | 8.34    | 0.5485667                 | 2.5151089                 | 103.26                              |
| NGC_6325     | 259.496327 | -23.767677 | 7.53          | 8.00    | -12.0979298               | 1.7598877                 | 66.36                               |
| NGC_6293     | 257.542500 | -26.582083 | 9.19          | 7.83    | -3.0115925                | -3.2291540                | -159.04                             |
| NGC_6266     | 255.304153 | -30.113390 | 6.03          | 7.32    | -5.4375876                | 2.1811825                 | 52.46                               |
| NGC_6139     | 246.918466 | -38.848782 | 10.04         | 6.94    | -6.1475598                | 2.5548822                 | 123.74                              |
| NGC_6539     | 271.207276 | -7.585858  | 8.16          | 6.78    | -6.4126601                | 4.3415298                 | 171.03                              |
| NGC_6517     | 270.460750 | -8.958778  | 9.23          | 6.76    | -4.6483533                | -0.7924843                | -38.58                              |
| NGC_6316     | 259.155417 | -28.140111 | 11.15         | 5.76    | -6.6254312                | 1.4319090                 | 85.36                               |
| IC_1276      | 272.684441 | -7.207595  | 4.55          | 5.67    | -5.2491931                | 0.0734359                 | 16.89                               |
| NGC_6355     | 260.993533 | -26.352827 | 8.65          | 5.43    | -3.1045387                | 3.6145579                 | 129.12                              |

## Continued

|           |            |            |       |       |             |            |         |
|-----------|------------|------------|-------|-------|-------------|------------|---------|
| NGC_6304  | 258.634399 | -29.462028 | 6.15  | 5.38  | -3.2467442  | 2.6895913  | 67.94   |
| NGC_5927  | 232.002869 | -50.673031 | 8.27  | 4.86  | -5.9737147  | 0.2206639  | -0.19   |
| NGC_5946  | 233.869051 | -50.659713 | 9.64  | 4.19  | -5.2698419  | 1.7848184  | 91.45   |
| NGC_6401  | 264.652191 | -23.909605 | 7.44  | 3.98  | -0.2254790  | 3.1178677  | 102.45  |
| NGC_6440  | 267.220167 | -20.360417 | 8.25  | 3.80  | -4.0480299  | -1.0291697 | -44.79  |
| Gran_3    | 256.256000 | -35.496000 | 11.47 | 3.42  | -1.9279856  | 3.3706196  | 188.73  |
| NGC_6256  | 254.886107 | -37.120968 | 7.24  | 3.31  | -3.5584548  | 1.8938272  | 59.18   |
| Pal_10    | 289.508728 | 18.571667  | 8.94  | 2.72  | -8.3622493  | 0.4888675  | 19.20   |
| Ter_2     | 261.887917 | -30.802333 | 7.75  | 2.30  | -6.3915840  | -1.6914029 | -56.78  |
| HP_1      | 262.771667 | -29.981667 | 7     | 2.12  | -7.0349280  | -7.5988281 | -250.68 |
| Gran_5    | 267.228000 | -24.170000 | 4.91  | 1.84  | -10.7390778 | -0.2004053 | -6.55   |
| Pal_6     | 265.925812 | -26.224995 | 7.05  | 1.78  | -9.3142921  | 5.0606473  | 174.65  |
| Ter_5     | 267.020200 | -24.779055 | 6.62  | 1.69  | -5.3372357  | -1.0392659 | -35.03  |
| Ter_4     | 262.662506 | -31.595528 | 7.59  | 1.31  | -6.0171770  | 2.4625908  | 87.52   |
| Ter_1     | 263.946667 | -30.481778 | 5.67  | 0.99  | -5.6574964  | -0.1965494 | -4.29   |
| VVV-CL001 | 268.677083 | -24.014722 | 8.08  | 0.78  | -3.1906301  | 2.0647555  | 74.68   |
| UKS_1     | 268.613312 | -24.145277 | 15.58 | 0.76  | -3.0226820  | -0.6591470 | -47.92  |
| VVV-CL160 | 271.737500 | -20.011111 | 6.8   | 0.30  | -15.6280977 | -6.4001518 | -205.15 |
| MASS-GC01 | 272.090851 | -19.829723 | 3.37  | 0.10  | -2.1965477  | 0.3430014  | 5.42    |
| Liller_1  | 263.352333 | -33.389556 | 8.06  | -0.16 | -8.6757093  | 0.5495440  | 20.84   |
| MASS-GC02 | 272.402100 | -20.778889 | 5.5   | -0.62 | -4.7191882  | 0.7329487  | 20.06   |
| FSR_1716  | 242.625000 | -53.748889 | 7.43  | -1.59 | -9.2559262  | -3.5049283 | -122.63 |
| FSR_1735  | 253.044174 | -47.058056 | 9.08  | -1.85 | -4.0720036  | 2.5688345  | 112.85  |
| Ter_10    | 270.740833 | -26.066944 | 10.21 | -1.86 | -5.6075545  | 4.6487625  | 218.15  |
| Ter_9     | 270.411667 | -26.839722 | 5.77  | -1.99 | -7.7646098  | -1.9157936 | -54.78  |
| Ter_12    | 273.065833 | -22.741944 | 5.17  | -2.10 | -5.6765625  | 4.0026695  | 94.65   |
| Ter_6     | 267.693250 | -31.275389 | 7.27  | -2.16 | -8.9621555  | 0.4812281  | 11.41   |
| NGC_6544  | 271.833833 | -24.998222 | 2.58  | -2.20 | -17.3750724 | -7.0550301 | -84.80  |
| NGC_6749  | 286.314056 | 1.899756   | 7.59  | -2.21 | -6.6322304  | -0.1851090 | -4.41   |
| Djor_1    | 266.869583 | -33.066389 | 9.88  | -2.48 | -9.6932606  | -0.3274483 | 0.23    |
| Djor_2    | 270.454378 | -27.825819 | 8.76  | -2.51 | -2.2577978  | -2.1068361 | -80.91  |
| Lynga_7   | 242.765213 | -55.317776 | 7.9   | -2.80 | -7.6266323  | -2.5589874 | -96.65  |
| NGC_6553  | 272.322992 | -25.908067 | 5.33  | -3.03 | -0.2035342  | -0.5159640 | -13.01  |
| FSR_1758  | 262.800000 | -39.808000 | 11.09 | -3.29 | 0.5294556   | 3.7789394  | 185.42  |
| NGC_6540  | 271.535657 | -27.765286 | 5.91  | -3.31 | -4.2579551  | 1.8611737  | 53.04   |
| NGC_6380  | 263.618611 | -39.069530 | 9.61  | -3.42 | -3.9208846  | 0.0824420  | 3.84    |
| Ton_2     | 264.042000 | -38.556100 | 6.99  | -3.42 | -3.8553524  | 4.5830534  | 162.72  |

**Continued**

|              |            |            |       |        |             |             |         |
|--------------|------------|------------|-------|--------|-------------|-------------|---------|
| Patchick_126 | 256.410833 | -47.342222 | 8     | -3.83  | -8.3804896  | -0.2312930  | -0.61   |
| NGC_6453     | 267.715508 | -34.598477 | 10.07 | -3.87  | -5.0134890  | -3.1525475  | -143.55 |
| NGC_6760     | 287.800268 | 1.030466   | 8.41  | -3.92  | -3.7289854  | -0.6933552  | -27.43  |
| NGC_6522     | 270.891958 | -30.033974 | 7.29  | -3.93  | -4.3504848  | -5.3973421  | -185.16 |
| Gran_1       | 269.651000 | -32.020000 | 8.27  | -3.98  | -10.9776707 | 2.9971787   | 111.82  |
| NGC_6528     | 271.206697 | -30.055778 | 7.83  | -4.17  | -5.9878352  | -0.8433308  | -46.66  |
| BH_140       | 193.472915 | -67.177276 | 4.81  | -4.31  | -14.8882993 | 1.4003266   | 25.08   |
| NGC_6712     | 283.268021 | -8.705960  | 7.38  | -4.32  | -2.4494228  | -4.9969944  | -166.35 |
| NGC_6838     | 298.443726 | 18.779194  | 4     | -4.56  | -4.0304540  | 1.5758897   | 31.61   |
| NGC_6441     | 267.554413 | -37.051445 | 12.73 | -5.01  | -5.9319594  | -0.5151124  | -32.60  |
| BH_261       | 273.527500 | -28.635000 | 6.12  | -5.27  | -1.4567879  | -4.8480501  | -134.64 |
| NGC_6626     | 276.137039 | -24.869847 | 5.37  | -5.58  | -8.0707163  | -3.8364185  | -98.34  |
| NGC_6558     | 272.573974 | -31.764508 | 7.79  | -6.02  | -4.4996159  | -0.4322626  | 4.59    |
| NGC_6642     | 277.975957 | -23.475602 | 8.05  | -6.44  | -3.5592824  | -1.6037873  | -54.06  |
| NGC_6569     | 273.411667 | -31.826889 | 10.53 | -6.68  | -8.4187435  | 0.2319725   | 17.31   |
| NGC_6388     | 264.071777 | -44.735500 | 11.17 | -6.74  | -3.0005843  | -0.3197011  | -26.57  |
| Pal_8        | 280.377290 | -19.828858 | 11.32 | -6.80  | -5.9339544  | -0.7175484  | -33.56  |
| NGC_6638     | 277.733734 | -25.497473 | 9.78  | -7.15  | -4.7651555  | 0.4186629   | 18.20   |
| NGC_6352     | 261.371277 | -48.422169 | 5.54  | -7.17  | -4.8921400  | -0.6296243  | -0.74   |
| NGC_6656     | 279.099762 | -23.904749 | 3.3   | -7.55  | -0.6499270  | -11.3075781 | -155.93 |
| NGC_6624     | 275.918793 | -30.361029 | 8.02  | -7.91  | -6.1470558  | -3.2581853  | -130.32 |
| NGC_4833     | 194.891342 | -70.876503 | 6.48  | -8.02  | -8.4165855  | -0.7001526  | -49.48  |
| NGC_4372     | 186.439101 | -72.659084 | 5.71  | -9.88  | -6.7104895  | 2.6446347   | 57.59   |
| NGC_6496     | 269.765350 | -44.265945 | 9.64  | -10.01 | -9.6033491  | -1.6935433  | -52.84  |
| NGC_6637     | 277.846252 | -32.348084 | 8.9   | -10.27 | -7.4403317  | 2.0260546   | 75.70   |
| NGC_6717     | 283.775177 | -22.701473 | 7.52  | -10.90 | -5.8714507  | 0.7399592   | 20.20   |
| NGC_6541     | 272.009827 | -43.714889 | 7.61  | -11.19 | -7.7409477  | -4.2616948  | -119.10 |
| NGC_2808     | 138.012909 | -64.863495 | 10.06 | -11.25 | 0.4735823   | 0.9252551   | 23.09   |
| NGC_6652     | 278.940125 | -32.990723 | 9.46  | -11.38 | -6.1790648  | 3.1761098   | 158.54  |
| NGC_6397     | 265.175385 | -53.674335 | 2.48  | -11.96 | -13.6757610 | -11.6202306 | -137.57 |
| NGC_6681     | 280.803162 | -32.292110 | 9.36  | -12.51 | -3.7237616  | -3.2439020  | -187.53 |
| ESO_280-SC06 | 272.275000 | -46.423333 | 20.95 | -12.57 | -2.7963703  | -0.6078765  | -79.25  |

The table gives the orbital parameters of 164 Galactic GC as derived from the Gaia EDR3 proper motions and radial velocities. The table contains all confirmed Milky Way GC with proper motion and radial velocity information.

The majority of the 164 GC are located in the central part of the Galaxy, so we selected GC from the table according to the following parameters: GC with galac-

tic longitude  $l$  in the range  $0^\circ < l < 90^\circ$  and  $270^\circ < l < 360^\circ$  (cut off the part behind the Sun). Thus, out of 164, 151 GC remain in the table. Next, we selected GC with a galactic latitude of  $13^\circ > b > -13^\circ$  (92 GC) and separately, a distance to the Galactic plane from 1.4 kpc to -1.4 kpc (77 GC).

**Table 2.** The GC sample from the general table for the range of distances to the plane from -1.4 to 1.4 kpc contains 77 GCs.

| Name     | RA         | DEC        | $R_{sun}$ kpc | $RV$ km/s | $\mu_b$ [mas yr <sup>-1</sup> ] | $Dp$ /kpc | $V_{\uparrow}, V_{\downarrow}$ km/s |
|----------|------------|------------|---------------|-----------|---------------------------------|-----------|-------------------------------------|
| NGC_6273 | 255.657486 | -26.267971 | 8.34          | 145.54    | 3.6079414229                    | 1.360     | 165                                 |
| NGC_6342 | 260.291573 | -19.587659 | 8.01          | 115.75    | -1.4921814347                   | 1.353     | -36                                 |
| NGC_6293 | 257.542500 | -26.582083 | 9.19          | -143.66   | -3.2291539667                   | 1.253     | -159                                |
| Ter_3    | 247.162483 | -35.339829 | 7.64          | -135.76   | 2.8935818900                    | 1.221     | 82                                  |
| NGC_6139 | 246.918466 | -38.848782 | 10.04         | 24.41     | 2.5548821981                    | 1.213     | 124                                 |
| NGC_6535 | 270.960449 | -0.297639  | 6.36          | -214.85   | 2.3670136697                    | 1.152     | 31                                  |
| NGC_6316 | 259.155417 | -28.140111 | 11.15         | 99.65     | 1.4319090063                    | 1.120     | 85                                  |
| NGC_6517 | 270.460750 | -8.958778  | 9.23          | -35.06    | -0.7924842869                   | 1.087     | -39                                 |
| NGC_6325 | 259.496327 | -23.767677 | 7.53          | 29.54     | 1.7598877255                    | 1.048     | 66                                  |
| NGC_6539 | 271.207276 | -7.585858  | 8.16          | 35.19     | 4.3415298028                    | 0.963     | 171                                 |
| NGC_6366 | 261.934357 | -5.079861  | 3.44          | -120.65   | -2.2913000101                   | 0.950     | -69                                 |
| NGC_6355 | 260.993533 | -26.352827 | 8.65          | -195.85   | 3.6145578895                    | 0.818     | 129                                 |
| NGC_6266 | 255.304153 | -30.113390 | 6.03          | -73.98    | 2.1811824878                    | 0.768     | 52                                  |
| NGC_3201 | 154.403427 | -46.412476 | 4.74          | 495.38    | 3.0374464690                    | 0.712     | 142                                 |
| NGC_5946 | 233.869051 | -50.659713 | 9.64          | 137.6     | 1.7848183790                    | 0.704     | 91                                  |
| NGC_5927 | 232.002869 | -50.673031 | 8.27          | -104.09   | 0.2206639186                    | 0.701     | 0                                   |
| Gran_3   | 256.256000 | -35.496000 | 11.47         | 94.87     | 3.3706196353                    | 0.685     | 189                                 |
| NGC_6304 | 258.634399 | -29.462028 | 6.15          | -108.62   | 2.6895912823                    | 0.576     | 68                                  |
| NGC_6440 | 267.220167 | -20.360417 | 8.25          | -69.39    | -1.0291696623                   | 0.547     | -45                                 |
| NGC_6401 | 264.652191 | -23.909605 | 7.44          | -105.44   | 3.1178677174                    | 0.516     | 102                                 |
| NGC_6121 | 245.896744 | -26.525749 | 1.85          | 71.22     | -3.5435439040                   | 0.509     | -10                                 |
| IC_1276  | 272.684441 | -7.207595  | 4.55          | 155.06    | 0.0734358716                    | 0.449     | 17                                  |
| Pal_10   | 289.508728 | 18.571667  | 8.94          | -31.7     | 0.4888674927                    | 0.425     | 19                                  |
| NGC_6256 | 254.886107 | -37.120968 | 7.24          | -99.75    | 1.8938272225                    | 0.418     | 59                                  |
| Ter_2    | 261.887917 | -30.802333 | 7.75          | 133.46    | -1.6914029127                   | 0.311     | -57                                 |
| HP_1     | 262.771667 | -29.981667 | 7             | 39.76     | -7.5988280550                   | 0.258     | -251                                |
| Pal_6    | 265.925812 | -26.224995 | 7.05          | 177       | 5.0606473239                    | 0.219     | 175                                 |
| UKS_1    | 268.613312 | -24.145277 | 15.58         | 59.38     | -0.6591469714                   | 0.208     | -48                                 |
| Ter_5    | 267.020200 | -24.779055 | 6.62          | -81.97    | -1.0392659446                   | 0.195     | -35                                 |
| Ter_4    | 262.662506 | -31.595528 | 7.59          | -48.96    | 2.4625907937                    | 0.173     | 88                                  |
| Gran_5   | 267.228000 | -24.170000 | 4.91          | -58.87    | -0.2004052860                   | 0.158     | -7                                  |

**Continued**

|              |            |            |       |         |                |        |      |
|--------------|------------|------------|-------|---------|----------------|--------|------|
| VVV-CL001    | 268.677083 | -24.014722 | 8.08  | -327.28 | 2.0647554734   | 0.110  | 75   |
| Ter_1        | 263.946667 | -30.481778 | 5.67  | 57.55   | -0.1965494344  | 0.098  | -4   |
| VVV-CL160    | 271.737500 | -20.011111 | 6.8   | 245.28  | -6.4001518435  | 0.036  | -205 |
| MASS-GC01    | 272.090851 | -19.829723 | 3.37  | -35.58  | 0.3430013522   | 0.006  | 5    |
| Liller_1     | 263.352333 | -33.389556 | 8.06  | 60.36   | 0.5495440375   | -0.023 | 21   |
| MASS-GC02    | 272.402100 | -20.778889 | 5.5   | -87.5   | 0.7329486715   | -0.059 | 20   |
| NGC_6544     | 271.833833 | -24.998222 | 2.58  | -38.46  | -7.0550300926  | -0.099 | -85  |
| Ter_12       | 273.065833 | -22.741944 | 5.17  | 94.01   | 4.0026694574   | -0.190 | 95   |
| Ter_9        | 270.411667 | -26.839722 | 5.77  | 68.56   | -1.9157935705  | -0.200 | -55  |
| FSR_1716     | 242.625000 | -53.748889 | 7.43  | -30.7   | -3.5049282823  | -0.206 | -123 |
| Ter_6        | 267.693250 | -31.275389 | 7.27  | 137.15  | 0.4812280920   | -0.274 | 11   |
| NGC_6553     | 272.322992 | -25.908067 | 5.33  | -0.27   | -0.5159639546  | -0.282 | -13  |
| NGC_6749     | 286.314056 | 1.899756   | 7.59  | -58.44  | -0.1851090091  | -0.292 | -4   |
| FSR_1735     | 253.044174 | -47.058056 | 9.08  | -69.85  | 2.5688344515   | -0.294 | 113  |
| NGC_6838     | 298.443726 | 18.779194  | 4     | -22.72  | 1.5758897311   | -0.318 | 32   |
| Ter_10       | 270.740833 | -26.066944 | 10.21 | 211.37  | 4.6487625204   | -0.332 | 218  |
| NGC_6540     | 271.535657 | -27.765286 | 5.91  | -16.5   | 1.8611736763   | -0.342 | 53   |
| BH_140       | 193.472915 | -67.177276 | 4.81  | 90.3    | 1.4003266259   | -0.361 | 25   |
| Djor_2       | 270.454378 | -27.825819 | 8.76  | -149.75 | -2.1068361326  | -0.383 | -81  |
| Lynga_7      | 242.765213 | -55.317776 | 7.9   | 17.86   | -2.5589874141  | -0.386 | -97  |
| Ton_2        | 264.042000 | -38.556100 | 6.99  | -184.72 | 4.5830533729   | -0.417 | 163  |
| Djor_1       | 266.869583 | -33.066389 | 9.88  | -359.18 | -0.3274483325  | -0.428 | 0    |
| NGC_6656     | 279.099762 | -23.904749 | 3.3   | -148.72 | -11.3075780998 | -0.434 | -156 |
| NGC_6522     | 270.891958 | -30.033974 | 7.29  | -15.23  | -5.3973420677  | -0.499 | -185 |
| NGC_6397     | 265.175385 | -53.674335 | 2.48  | 18.51   | -11.6202306433 | -0.514 | -138 |
| NGC_6626     | 276.137039 | -24.869847 | 5.37  | 11.11   | -3.8364185245  | -0.522 | -98  |
| Patchick_126 | 256.410833 | -47.342222 | 8     | -122.14 | -0.2312929821  | -0.534 | -1   |
| NGC_6712     | 283.268021 | -8.705960  | 7.38  | -107.45 | -4.9969944420  | -0.556 | -166 |
| BH_261       | 273.527500 | -28.635000 | 6.12  | -60     | -4.8480501092  | -0.562 | -135 |
| NGC_6528     | 271.206697 | -30.055778 | 7.83  | 211.86  | -0.8433307918  | -0.570 | -47  |
| Gran_1       | 269.651000 | -32.020000 | 8.27  | 78.94   | 2.9971787050   | -0.574 | 112  |
| NGC_6380     | 263.618611 | -39.069530 | 9.61  | -1.48   | 0.0824420498   | -0.574 | 4    |
| NGC_6760     | 287.800268 | 1.030466   | 8.41  | -2.37   | -0.6933551606  | -0.576 | -27  |
| FSR_1758     | 262.800000 | -39.808000 | 11.09 | 227.31  | 3.7789394057   | -0.637 | 185  |
| NGC_6453     | 267.715508 | -34.598477 | 10.07 | -99.23  | -3.1525475223  | -0.680 | -144 |
| NGC_6352     | 261.371277 | -48.422169 | 5.54  | -125.63 | -0.6296242777  | -0.691 | -1   |
| NGC_6558     | 272.573974 | -31.764508 | 7.79  | -195.12 | -0.4322626027  | -0.817 | 5    |

## Continued

|          |            |            |       |        |               |        |      |
|----------|------------|------------|-------|--------|---------------|--------|------|
| NGC_6642 | 277.975957 | -23.475602 | 8.05  | -60.61 | -1.6037873078 | -0.903 | -54  |
| NGC_4833 | 194.891342 | -70.876503 | 6.48  | 201.99 | -0.7001526401 | -0.904 | -49  |
| NGC_4372 | 186.439101 | -72.659084 | 5.71  | 75.59  | 2.6446347474  | -0.980 | 58   |
| NGC_6624 | 275.918793 | -30.361029 | 8.02  | 54.79  | -3.2581853134 | -1.104 | -130 |
| NGC_6441 | 267.554413 | -37.051445 | 12.73 | 18.47  | -0.5151123783 | -1.111 | -33  |
| NGC_6638 | 277.733734 | -25.497473 | 9.78  | 8.63   | 0.4186628947  | -1.218 | 18   |
| NGC_6569 | 273.411667 | -31.826889 | 10.53 | -49.83 | 0.2319725137  | -1.225 | 17   |
| NGC_6388 | 264.071777 | -44.735500 | 11.17 | 83.11  | -0.3197010757 | -1.311 | -27  |
| Pal_8    | 280.377290 | -19.828858 | 11.32 | -39.68 | -0.7175484457 | -1.340 | -34  |

## 2.1. Dependence of GC Velocities $V_{\uparrow}$ and $V_{\downarrow}$ on Galactic Latitude $B$

The sample for  $13^{\circ} > b > -13^{\circ}$  consists of 92 GC (**Table 1**) In the original table, [7] the following GC parameters are given:

- $RA$ : Right ascension
- $DEC$ : Declination
- $l$ : Galactic longitude
- $b$ : Galactic latitude
- $R_{\odot}$ : Distance from Sun
- $RGC$ : Distance from the Galactic center
- $RV$ : Radial velocity
- $\mu_{\alpha\cos\delta}$ : Proper motion in right ascension
- $\mu_{\delta}$ : Proper motion in declination
- $\rho_{\mu\alpha\mu\delta}$ : Correlation coefficient
- $X$ : Distance from the Gal. center in direction of Sun
- $Y$ : Distance from the Gal. center in direction of Solar motion
- $Z$ : Distance above/below galactic plane
- $U$ : Velocity in  $X$  direction
- $V$ : Velocity in  $Y$  direction
- $W$ : Velocity in  $Z$  direction
- $RPeri$ : Average perigalactic distance
- $RApo$ : Average apogalactic distance

As stated in the article [7] distances  $R_{\odot}$  to GC are determined either by using eclipsing binaries [8] [9] or through fits of their color-magnitude diagrams (CMDs) with theoretical isochrones e.g. [10]-[13], by using variable stars that follow known relations between their periods and absolute luminosities like RR Lyrae stars e.g. [14] [15] Type II Cepheid [16] or Mira type variables [17]. Finally, it is possible to determine distances by comparing the magnitudes of main-sequence stars with stars of similar metallicity in the solar neighborhood, the so-called subdwarf method e.g. [18] [19] or kinematically by comparing line-of-sight and proper motion velocity dispersion profiles in GC e.g. [20]-[22]. The latter method has the advantage that the derived distance is not influenced by the reddening of

the cluster. For GC with accurately measured radial velocities and dispersion of proper motions, the distance to the GC can be determined by achieving a better fit with a theoretical cluster model e.g. [23].

RV radial velocities were calculated by [24] by combining literature data with ESO and Keck data archives. [25] also added radial velocities from Gaia DR2 and the Anglo-Australian Observatory (AAO) to the table. The radial velocities given in [26] were also added based on MUSE data. Own motions were added to the table from Gaia EDR3 or HST.

For this work, we used the following table parameters:  $RA$ ,  $DEC$ ,  $l$ ,  $b$ ,  $RGC$ ,  $\mu\alpha\cos\delta$ ,  $\mu\delta$ ,  $Z$  and  $W$ .

The method for determining the velocity of the GC movement relative to the plane and center of the Galaxy is as follows: we find the position of the GC today (or rather at the time of observation) and in 1 year. The difference between these GC positions gives the velocity of movement for 1 year. Next, we convert this result into km/s. Although the parameters  $l$ ,  $b$ ,  $RGC$ ,  $Z$  and  $W$  are given in the original table, in order to use the same calculation tools for the two GC positions, we recalculate them using the corresponding formulas.

We obtain  $l$  and  $b$  ourselves by converting coordinates using the formulas:

$$\sin(b) = \sin(\delta_{NGP}) * \sin(\delta) + \cos(\delta_{NGP}) * \cos(\delta) * \cos(\alpha - \alpha_{NGP}) \quad (1)$$

$$\tan(l_{NCP} - l) = \frac{\cos(\delta) * \sin(\alpha - \alpha_{NGP})}{\sin(\delta) * \cos(\delta_{NGP}) - \cos(\delta) * \sin(\delta_{NGP}) * \cos(\alpha - \alpha_{NGP})} \quad (2)$$

where:

- $\alpha$  and  $\delta$ : equatorial coordinates of the GC,
- $\delta_{NGP}$  and  $\alpha_{NGP}$  are the equatorial coordinates of the north galactic pole,
- $l_{NCP}$ : Galactic longitude of the North celestial pole,
- $l$  and  $b$  are the galactic coordinates of the GC.

The proper motions  $\mu l$ ,  $\mu b$  were calculated based on  $\mu\alpha$ ,  $\mu\delta$  as follows: first,  $l$  and  $b$  are calculated based on the above formulas and then  $l'$  and  $b'$  (GC galactic coordinates in a year) using  $\alpha' = \alpha + \mu\alpha$  and  $\delta' = \delta + \mu\delta$ . Next we get  $\mu l = l' - l$ ,  $\mu b = b' - b$ .

Using  $\mu b$ , we obtain the velocity of movement  $V\uparrow$  of the GC in the northern region relative to the Galaxy plane according to the formula:

$$V\uparrow = (R_{\odot} + RV * SY/K) * \sin(b + \mu b) - R_{\odot} * \sin(b) \quad \text{where:}$$

- $R_{\odot}$ : Distance from the Sun
- $RV$ : Radial velocity of GC
- $SY$ : seconds in a year
- $K$ : km in kpc

Thus, we obtained the velocities  $V\uparrow$  of the GC motion in the direction orthogonal to the galactic plane. We, then sorted them in **Table 1** in descending order of  $b$ . For the southern region of the Galaxy, we will do the same with negative values of the indicated ranges  $b$  and denote the velocities  $V\downarrow$ . **Figure 1** and **Figure 2** show the GC velocities  $V\uparrow$  and  $V\downarrow$  in the northern and southern regions of the Galaxy.

Thus, it can be argued that the GCs of the northern region in the range  $0^\circ < b < 13^\circ$  on average move away from the Galactic plane. The average velocity of the GC's receding from the Galactic plane in the northern region is  $30.36 \pm 15.29$  km/s ( $N = 42$ ). Similarly, GCs in the southern region of the Galaxy in the range  $-13^\circ < b < 0^\circ$  on average move away from the Galactic plane at a velocity of  $17.85 \pm 13.76$  km/s ( $N = 50$ ).

Applying Student's t-test shows that the GC velocities  $V_\uparrow$  and  $V_\downarrow$  of the northern and southern regions of the Galaxy in the ranges  $0^\circ < b < 13^\circ$  and  $-13^\circ < b < 0^\circ$  differ at the level of 0.0205.

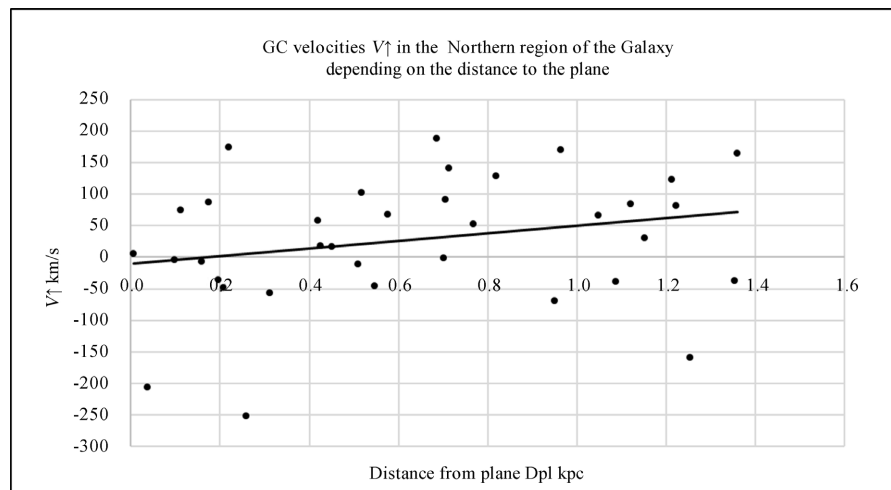


**Figure 3.** GC velocities  $V_\uparrow$  in the northern region of the Galaxy depending on the distance to the Galactic plane. As can be seen from the figure, most GCs have a positive velocity, *i.e.* moving away from the galactic plane.

## 2.2. GC Velocities $V_\uparrow$ and $V_\downarrow$ Relative to the Galactic Plane Depending on the Distance to the Plane

In the previous section, we obtained the GC movement velocities depending on the galactic latitude  $b$ . Now let's move on to determining the GC velocities relative to the distance to the Galactic plane ( $Dpl$ ). The GC sample from the general table for the range of distances to the plane from  $-1.4$  to  $1.4$  kpc contains 77 GCs (Table 2). GC velocities  $V_\uparrow$  and  $V_\downarrow$  for the northern and southern regions of the Galaxy are shown in Figure 3 and Figure 4.

On average, the GCs of the northern and southern regions of the Galaxy move away from the Galactic plane. The average velocity of the GCs receding from the plane for the northern region of the Galaxy is  $27.74 \pm 17.13$  km/s ( $N = 35$ ) and for the southern region  $-17.41 \pm 14.51$  km/s ( $N = 42$ ). Applying Student's t-test shows that the GC velocities  $V_\uparrow$  and  $V_\downarrow$  of the northern and southern regions of the Galaxy for the distance ranges from the plane  $0 < Dpl < 1.4$  kpc and  $-1.4 < Dpl < 0$  kpc differ at the level of 0.0496.

It should be noted that similar results are obtained if we use the data from the original table:  $Z$  (Distance to the plane) and  $W$  (Velocity in  $Z$  direction) (Figure

5 and Figure 6). The difference in velocities  $V\uparrow$  and  $V\downarrow$  from the tabular data  $W$  is approximately 7.24 km/s, which can be attributed to the oscillation of the solar orbit ([27]-[32]).

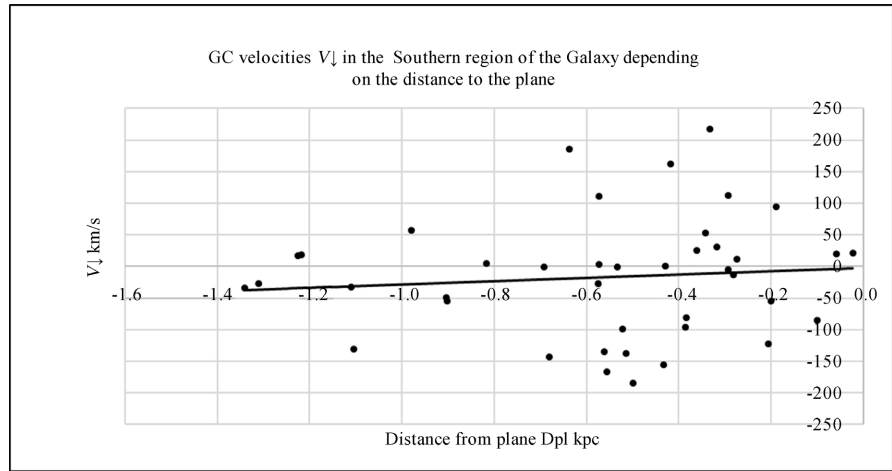


**Figure 4.** GC velocities  $V\downarrow$  in the southern region of the Galaxy depending on the distance to the Galactic plane  $Dpl$ . Most GCs have a negative velocity, *i.e.* move away from the plane.

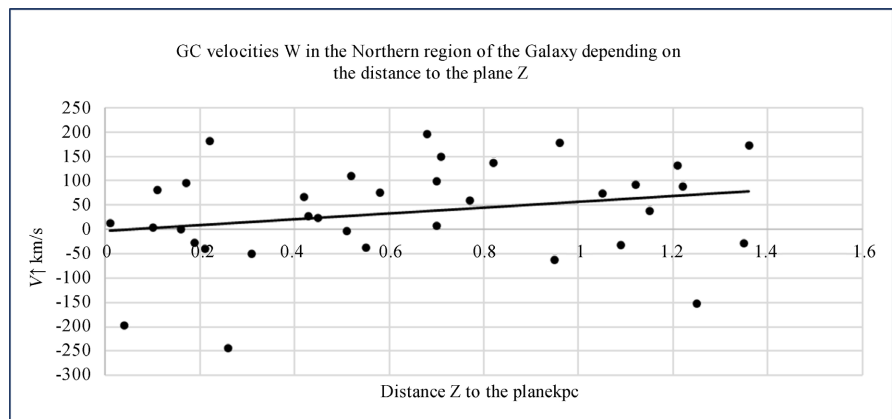


**Figure 5.** GC velocities  $W$  in the northern region of the Galaxy depending on the distance  $Z$  to the Galactic plane. Most GCs have a positive velocity, *i.e.* move away from the plane.

The dependence of the GC velocities  $V\uparrow$  and  $V\downarrow$  over the entire range  $-1.4 < Dpl < 1.4$  kpc is shown in Figure 7. As can be seen from the figure, there is an obvious dependence between the parameters discussed. Let us evaluate the significance of the correlation. To do this, we use the value

$$t = R \sqrt{\frac{n-2}{1-R^2}} \tag{3}$$

which obeys the Student distribution. Here,

$$R(V, Dpl) = \frac{\sum (V_i - \langle V \rangle)(D_{pli} - \langle D_{pl} \rangle)}{(n-1)\sigma_V \sigma_{Dpl}} \tag{4}$$

- assessment of the correlation between the values of  $V$  and  $D_{pl}$ ,  $\sigma_V$  and  $\sigma_{D_{pl}}$ : standard deviations of the corresponding values.

$$\sigma_V = \sqrt{\frac{\sum_{i=0}^n (V_i - \langle V \rangle)^2}{n-1}}, \quad \sigma_{D_{pl}} = \sqrt{\frac{\sum_{i=0}^n (D_{pl}_i - \langle D_{pl} \rangle)^2}{n-1}}, \quad (5)$$

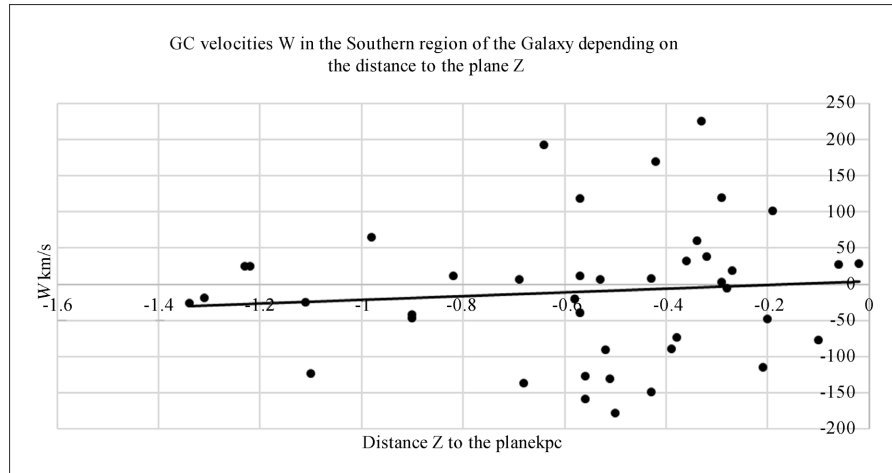


**Figure 6.** GC velocities  $W$  in the southern region of the Galaxy depending on the distance to the Galactic plane  $Z$ . Most GCs have a negative velocity, *i.e.* move away from the plane.

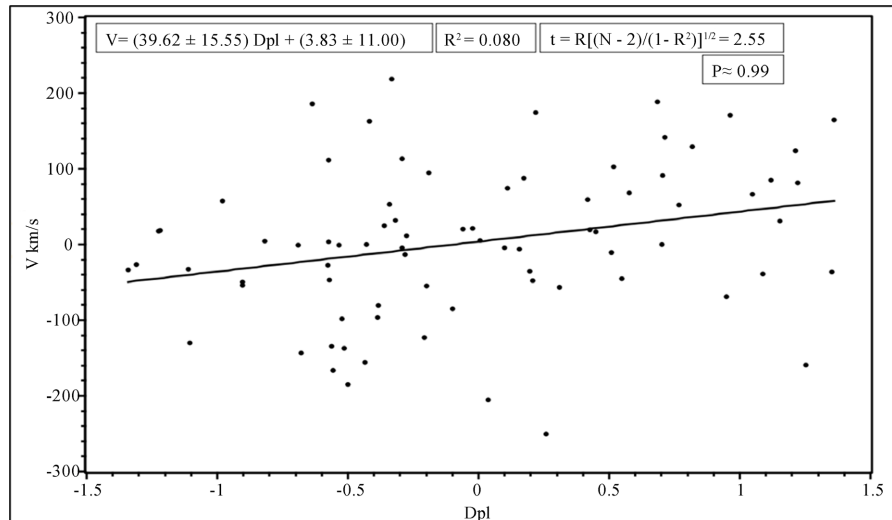


**Figure 7.** Dependence of GC velocities in the direction perpendicular to the Galactic plane on the distance of the GC to the plane for the entire range  $-1.4$  to  $1.4$  kpc.

We get  $t = 2.55$ , from which it follows that the significance of the correlation is high  $\alpha = 1 - P \approx 0.01$ . Thus, we can conclude that GCs far from the Galactic plane, on average, have relatively high speeds of receding from the Galactic plane.

### 2.3. Factor of Spatial and Kinematic Symmetry of GC

**Figure 8** shows the plot of GC by distance  $Z$  from the galactic plane versus the velocities  $W$  at a distance of up to 4 kpc. As can be seen from the figure, GCs are

distributed quite symmetrically along the  $Z$  axis. Visually, it seems that the GCs are also distributed symmetrically by velocities  $W$ . In fact, the velocities of the northern and southern GCs differ significantly. The GC of the northern region is 23.02 km/s, and of the southern region - 10.48 km/s. The asymmetry value  $Asm = 12.54$  km/s. We assume that this is due to the oscillation of the solar orbit (about 7 km/s relative to the plane). It is logical to accept that in order to obtain spatial symmetry, it is necessary to have symmetry by velocities as well, otherwise, over the past billions of years, spatial symmetry would have been broken.

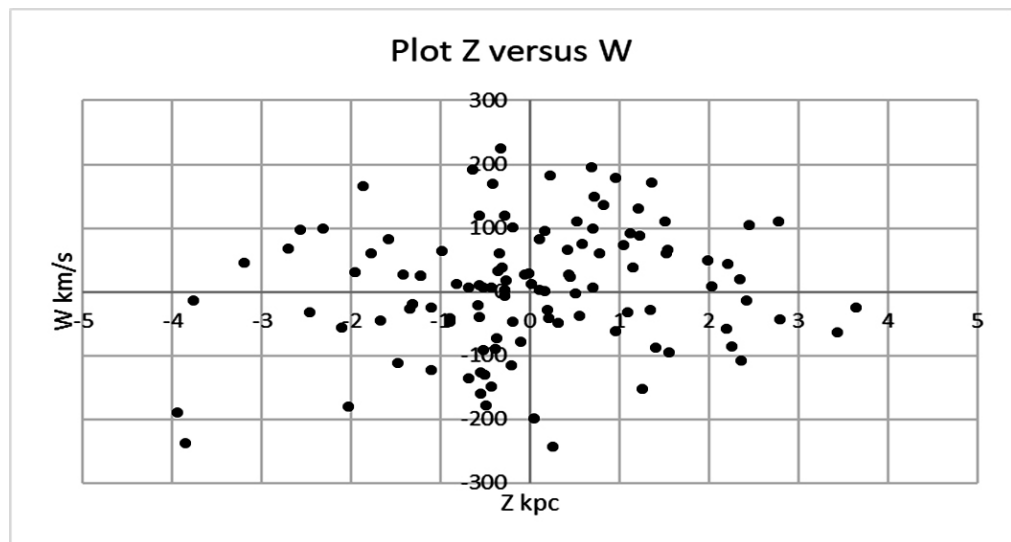


**Figure 8.** Plot Z versus W. We can see visual symmetry in Z direction.

#### 2.4. GC Motion Relative to the Galactic Center

The result obtained in the previous sections that GCs on average move away from the Galactic plane suggests that it is possible that GCs on average can also move away from the Galactic center, so this work attempts to test this assumption.

Using the table data from 151 GCs, the distances of the GC from the center of the Galaxy  $R_{gal}$  (Galactocentric distances) and the velocity of movement of the GC ( $VR$ ) relative to the center of the Galaxy were calculated (it should be noted that this data is not in the original table). To do this, we calculated the distance of each GC from the center of the Galaxy for two points of location of these GCs: the “current” (or rather at the moment of observation) distance of the GC from the center  $R_{gal}$  (Galactocentric distance) and the distance calculated after a 1 year  $R'_{gal}$ . The difference between these distances gives us the velocity of movement of the GC relative to the center, *i.e.*  $VR = R'_{gal} - R_{gal}$ . In the table, the current distance of the GC from the center of the Galaxy  $R_{GC}$  is given rounded to the second decimal number, so we considered it appropriate to calculate these values ourselves. Using simple trigonometry, the velocities of globular clusters relative to the center of the Galaxy are calculated. The current distance of the GC from the Galactic center is calculated using the following formula:

$$R_{gal} = \sqrt{(D_{CL} * \sin(b))^2 + (D_{GC} * \sin(l))^2 + (D_{CL} * \cos(b) - D_{GC} * \cos(l))^2} \quad (6)$$

where:

- $D_{GC}$  (kpc): distance from the Sun to the center of the Galaxy;
- $b$  : galactic latitude of the Globular Cluster (GC);
- $l$  : galactic longitude of the Globular Cluster (GC);
- $D_{Cl}$  : distance from the Sun to the center of the GC;
- $R_{gal}$  : distance from the center of the Galaxy to the center of the GC.

The distance of the GC from the Galactic center in 1 year is calculated using the following formula:

$$R'_{gal} = \sqrt{(D'_{CL} * \sin(b'))^2 + (D_{GC} * \sin(l'))^2 + (D'_{CL} * \cos(b') - D_{GC} * \cos(l'))^2} \quad (7)$$

where:

- $D'_{Cl} = D_{Cl} + RV$  distance from the Sun to the GC in a year;
- $b' = b + \mu b$  : galactic latitude in a year;
- $l' = l + \mu l$  : galactic longitude in a year;
- $RV$ : radial velocity of the GC relative to the Sun.

The average velocity of the GC relative to the Galactic center for the range 0 to 12 kpc is  $31.70 \pm 14.74$  km/s ( $N = 119$ ). At the same time, with increasing distance this speed decreases and for a distance of 90 kpc it reaches about 9 km/s, which can be attributed to the gravitational influence of the galaxy on the GC. Based on the calculations obtained, it can be assumed that GCs, on average, are probably also moving away from the Galactic center.

### 3. Conclusion and Discussion

Thus, within the framework of this work, the velocities of movement  $V_{\uparrow}$  and  $V_{\downarrow}$  of the globular clusters of the northern and southern regions of the Galaxy were calculated depending on the Galactic latitude  $b$  and the distance to the Galactic plane. The GC motion velocities relative to the Galactic center were also calculated. The following results were obtained:

- GCs of the northern region in the range  $0^\circ < b < 13^\circ$  on average move away from the Galactic plane. The average velocity of the GC's receding from the Galactic plane in the northern region is  $30.36 \pm 15.29$  km/s ( $N = 42$ ).
- GCs in the southern region of the Galaxy in the range  $-13^\circ < b < 0^\circ$  on average move away from the Galactic plane at a velocity of  $17.85 \pm 13.76$  km/s ( $N = 50$ ).
- GCs in the northern region of the Galaxy in the range of distances to the plane from 0 to 1.4 kpc on average move away from the plane of the Galaxy. The average velocity of receding of the GC in the northern region from the Galactic plane is  $27.74 \pm 17.13$  km/s ( $N = 35$ ).
- GCs in the southern region of the Galaxy in the range of distances to the plane from 0 to 1.4 kpc on average move away from the plane of the Galaxy. The average velocity of receding of the GC in the southern region from the Galactic plane is

$17.41 \pm 14.51$  km/s ( $N = 42$ ).

- The average velocity of receding of the GC from the Galactic center for the range 0 to 12 kpc is  $31.70 \pm 14.74$  km/s ( $N = 119$ ) and decreases with increasing distance.

Thus, it can be stated that the population of the second type of Galaxy, using the example of Globular clusters, at least in the central part, is possibly expanding, which gives reason to assume that the Galaxy itself is also expanding within the specified limits. By accepting this idea, we can calculate the sizes of galaxies depending on their age, for example, if the expansion speed is 10 km/s, then in a billion years the size of the galaxy will be approximately 20 kpc, which is quite consistent with the average galaxy size. The latter suggests that the accepted age of our galaxy should possibly be revised. This seems unlikely as it is not consistent with current theory, so it can be considered a preliminary result requiring further study both theoretically and observationally.

Acceptance of this idea can explain the discrepancy between the ages of our galaxy and the massive galaxies discovered by the James Webb Space Telescope (JWST) [33], whose age is estimated to be less than 1 billion years. Refinement of the results obtained and further research will be facilitated by the presence of a larger number of studied clusters with more accurate parameters.

## Data Availability

For the research in this paper, we used the table of 164 well-studied Globular clusters of the Milky Way Galaxy given by [7]. The table gives the orbital parameters of Galactic globular clusters as derived from the Gaia proper motions and radial velocities. The table contains all confirmed Milky Way globular clusters with proper motion and radial velocity information. The distances and the other parameters of Galactic globular clusters can be obtained from the following webpage: <https://people.smp.uq.edu.au/HolgerBaumgardt/globular/orbits.html>.

## Acknowledgements

We are grateful to Holger Baumgardt for a thoughtful discussion of the results of this work.

## Conflicts of Interest

The authors declare no conflicts of interest regarding the publication of this paper.

## References

- [1] Martínez-Lombilla, C., Trujillo, I. and Knapen, J.H. (2019) Discovery of Disc Truncations above the Galaxies' Mid-Plane in Milky Way-Like Galaxies. *Monthly Notices of the Royal Astronomical Society*, **483**, 664-691. <https://doi.org/10.1093/mnras/sty2886>
- [2] Chen, S., Richer, H., Caiazzo, I. and Heyl, J. (2018) Distances to the Globular Clusters 47 Tucanae and NGC 362 Using *Gaia* DR2 Parallaxes. *The Astrophysical Journal*, **867**, Article 132. <https://doi.org/10.3847/1538-4357/aae089>

- [3] Shao, Z. and Li, L. (2019) *Gaia* Parallax of Milky Way Globular Clusters—A Solution of Mixture Model. *Monthly Notices of the Royal Astronomical Society*, **489**, 3093-3101. <https://doi.org/10.1093/mnras/stz2317>
- [4] Forveille, T., Kotak, R., Shore, S. and Tolstoy, E. (2018) *Gaia* Data Release 2. *Astronomy & Astrophysics*, **616**, E1. <https://doi.org/10.1051/0004-6361/201833955>
- [5] Vasiliev, E. and Baumgardt, H. (2021) *Gaia* EDR3 View on Galactic Globular Clusters. *Monthly Notices of the Royal Astronomical Society*, **505**, 5978-6002. <https://doi.org/10.1093/mnras/stab1475>
- [6] Vasiliev, E. (2019) Proper Motions and Dynamics of the Milky Way Globular Cluster System from *Gaia* DR2. *Monthly Notices of the Royal Astronomical Society*, **484**, 2832-2850. <https://doi.org/10.1093/mnras/stz171>
- [7] Baumgardt, H. and Vasiliev, E. (2021) Accurate Distances to Galactic Globular Clusters through a Combination of *Gaia* EDR3, *HST*, and Literature Data. *Monthly Notices of the Royal Astronomical Society*, **505**, 5957-5977. <https://doi.org/10.1093/mnras/stab1474>
- [8] Kaluzny, J., Thompson, I.B., Rozycka, M., Dotter, A., Krzeminski, W., Pych, W., *et al.* (2013) The Cluster Ages Experiment (Case). V. Analysis of Three Eclipsing Binaries in the Globular Cluster M4. *The Astronomical Journal*, **145**, Article 43. <https://doi.org/10.1088/0004-6256/145/2/43>
- [9] Thompson, I.B., Udalski, A., Dotter, A., Rozycka, M., Schwarzenberg-Czerny, A., Pych, W., *et al.* (2020) The Cluster Ages Experiment (CASE)-VIII. Age and Distance of the Globular Cluster 47 Tuc from the Analysis of Two Detached Eclipsing Binaries. *Monthly Notices of the Royal Astronomical Society*, **492**, 4254-4267. <https://doi.org/10.1093/mnras/staa032>
- [10] Ferraro, F.R., Montegriffo, P., Origlia, L. and Fusi Pecci, F. (2000) A New Infrared Array Photometric Survey of Galactic Globular Clusters: A Detailed Study of the Red Giant Branch Sequence as a Step toward the Global Testing of Stellar Models. *The Astronomical Journal*, **119**, 1282-1295. <https://doi.org/10.1086/301269>
- [11] Dotter, A., Sarajedini, A., Anderson, J., Aparicio, A., Bedin, L.R., Chaboyer, B., *et al.* (2009) The Acs Survey of Galactic Globular Clusters. IX. Horizontal Branch Morphology and the Second Parameter Phenomenon. *The Astrophysical Journal*, **708**, 698-716. <https://doi.org/10.1088/0004-637x/708/1/698>
- [12] Gontcharov, G.A., Mosenkov, A.V. and Khovritchev, M.Y. (2018) Isochrone Fitting of Galactic Globular Clusters—I. NGC 5904. *Monthly Notices of the Royal Astronomical Society*, **483**, 4949-4967. <https://doi.org/10.1093/mnras/sty3439>
- [13] Valcin, D., Bernal, J.L., Jimenez, R., Verde, L. and Wandelt, B.D. (2020) Inferring the Age of the Universe with Globular Clusters. *Journal of Cosmology and Astroparticle Physics*, **12**, Article 002. <https://doi.org/10.1088/1475-7516/2020/12/002>
- [14] Bono, G., Caputo, F. and Di Criscienzo, M. (2007) RR Lyrae Stars in Galactic Globular Clusters. *Astronomy & Astrophysics*, **476**, 779-790. <https://doi.org/10.1051/0004-6361:20078206>
- [15] Hernitschek, N., Cohen, J.G., Rix, H., Magnier, E., Metcalfe, N., Wainscoat, R., *et al.* (2019) Precision Distances to Dwarf Galaxies and Globular Clusters from Pan-STARRS1  $3\pi$  RR Lyrae. *The Astrophysical Journal*, **871**, Article 49. <https://doi.org/10.3847/1538-4357/aaf388>
- [16] Matsunaga, N., Fukushi, H., Nakada, Y., Tanabé, T., Feast, M.W., Menzies, J.W., *et al.* (2006) The Period-Luminosity Relation for Type II Cepheids in Globular Clusters. *Monthly Notices of the Royal Astronomical Society*, **370**, 1979-1990. <https://doi.org/10.1111/j.1365-2966.2006.10620.x>

- [17] Feast, M., Whitelock, P. and Menzies J. (2002) Globular Clusters and the Mira Period-Luminosity Relation. *MNRAS*, **370**, 1979-1990.
- [18] Reid, I.N. and Gizis, J.E. (1998) The Distance to NGC 6397 by M-Subdwarf Main-Sequence Fitting. *The Astronomical Journal*, **116**, 2929-2935. <https://doi.org/10.1086/300653>
- [19] Cohen, R.E., Sarajedini, A., Kinemuchi, K. and Leiton, R. (2010) The Unusual RR Lyrae Population of NGC 6101. *The Astrophysical Journal*, **727**, Article 9. <https://doi.org/10.1088/0004-637x/727/1/9>
- [20] McNamara, B.J., Harrison, T.E. and Baumgardt, H. (2004) The Dynamical Distance to M15: Estimates of the Cluster's Age and Mass and of the Absolute Magnitude of Its RR Lyrae Stars. *The Astrophysical Journal*, **602**, 264-270. <https://doi.org/10.1086/380905>
- [21] van de Ven, G., van den Bosch, R.C.E., Verolme, E.K. and de Zeeuw, P.T. (2006) The Dynamical Distance and Intrinsic Structure of the Globular Cluster  $\omega$  Centauri. *Astronomy & Astrophysics*, **445**, 513-543. <https://doi.org/10.1051/0004-6361:20053061>
- [22] Watkins, L.L., van der Marel, R.P., Bellini, A. and Anderson, J. (2015) *Hubble Space Telescope* Proper Motion (HSTPROMO) Catalogs of Galactic Globular Clusters. III. Dynamical Distances and Mass-to-Light Ratios. *The Astrophysical Journal*, **812**, Article 149. <https://doi.org/10.1088/0004-637x/812/2/149>
- [23] Hénault-Brunet, V., Gieles, M., Sollima, A., Watkins, L.L., Zocchi, A., Claydon, I., *et al.* (2019) Mass Modelling Globular Clusters in the Gaia era: A Method Comparison Using Mock Data from an  $N$ -Body Simulation of M 4. *Monthly Notices of the Royal Astronomical Society*, **483**, 1400-1425. <https://doi.org/10.1093/mnras/sty3187>
- [24] Baumgardt, H. and Hilker, M. (2018) A Catalogue of Masses, Structural Parameters, and Velocity Dispersion Profiles of 112 Milky Way Globular Clusters. *Monthly Notices of the Royal Astronomical Society*, **478**, 1520-1557. <https://doi.org/10.1093/mnras/sty1057>
- [25] Baumgardt, H., Hilker, M., Sollima, A. and Bellini, A. (2018) Mean Proper Motions, Space Orbits, and Velocity Dispersion Profiles of Galactic Globular Clusters Derived from Gaia DR2 Data. *Monthly Notices of the Royal Astronomical Society*, **482**, 5138-5155. <https://doi.org/10.1093/mnras/sty2997>
- [26] Kamann, S., Husser, T.-O., Dreizler, S., Emsellem, E., Weilbacher, P.M., Martens, S., *et al.* (2017) A Stellar Census in Globular Clusters with MUSE: The Contribution of Rotation to Cluster Dynamics Studied with 200 000 Stars. *Monthly Notices of the Royal Astronomical Society*, **473**, 5591-5616. <https://doi.org/10.1093/mnras/stx2719>
- [27] Gordon, D., de Witt, A. and Jacobs, C.S. (2023) Position and Proper Motion of Sagittarius A\* in the ICRF3 Frame from VLBI Absolute Astrometry. *The Astronomical Journal*, **165**, Article 49. <https://doi.org/10.3847/1538-3881/aca65b>
- [28] Reid, M.J. and Brunthaler, A. (2020) The Proper Motion of Sagittarius A\*. III. The Case for a Supermassive Black Hole. *The Astrophysical Journal*, **892**, Article 39. <https://doi.org/10.3847/1538-4357/ab76cd>
- [29] Xu, S., Zhang, B., Reid, M.J., Zheng, X., Wang, G. and Jung, T. (2022) A Milliarcsecond-Accurate Position for Sagittarius A\*. *The Astrophysical Journal*, **940**, Article 15. <https://doi.org/10.3847/1538-4357/ac98b9>
- [30] Francis, C. and Anderson, E. (2009) Calculation of the Local Standard of Rest from 20574 Local Stars in the New Hipparcos Reduction with Known Radial Velocities. *New Astronomy*, **14**, 615-629. <https://doi.org/10.1016/j.newast.2009.03.004>
- [31] Dehnen, W. and Binney, J.J. (1998) Local Stellar Kinematics from Hipparcos Data.

*Monthly Notices of the Royal Astronomical Society*, **298**, 387-394.

<https://doi.org/10.1046/j.1365-8711.1998.01600.x>

- [32] Schönrich, R., Binney, J. and Dehnen, W. (2010) Local Kinematics and the Local Standard of Rest. *Monthly Notices of the Royal Astronomical Society*, **403**, 1829-1833. <https://doi.org/10.1111/j.1365-2966.2010.16253.x>
- [33] Xiao, M., Oesch, P.A., Elbaz, D., Bing, L., Nelson, E.J., Weibel, A., *et al.* (2024) Accelerated Formation of Ultra-Massive Galaxies in the First Billion Years. *Nature*, **635**, 311-315. <https://doi.org/10.1038/s41586-024-08094-5>